Nuclear Instruments and Methods in Physics Research B 267 (2009) 167–170

Contents lists available at ScienceDirect

Nuclear Instruments and Methods in Physics Research B

journal homepage: www.elsevier.com/locate/nimb

Short Communication

# Energy dependence of electron stopping powers in elemental solids over the 100 eV to 30 keV energy range

K. Kumagai [a,*], S. Tanuma [b], C.J. Powell [c]

[a] Graduate School of Pure and Applied Science, University of Tsukuba, 1-1 Namiki, Tsukuba, Ibaraki 305-0044, Japan
[b] Materials Analysis Station, National Institute for Materials Science, 1-2-1 Sengen, Tsukuba, Ibaraki 305-0047, Japan
[c] Surface and Microanalysis Science Division, National Institute of Standards and Technology, Gaithersburg, MD 20899-8370, USA

ARTICLE INFO

*Article history:*
Received 9 October 2008
Received in revised form 30 October 2008
Available online 25 November 2008

*PACS:*
34.80.−i
72.10.−d

*Keywords:*
Electron stopping power
Fano plot
Elemental solids
Energy dependence

ABSTRACT

We analyzed the energy dependence of electron stopping powers (SPs) calculated for 41 elemental solids from experimental optical data for electron energies between 100 eV and 30 keV. Our analysis was performed with the Hill equation to represent a series of steps in plots of the slopes of Fano plots. The average root-mean-square difference between SPs from fits with an equation derived from the Hill equation and the calculated SPs was 1.0%. The new equation can provide SPs over a wide energy range for Monte Carlo simulations of electron transport with the continuous slowing-down approximation.



The electron stopping power (SP) is an important parameter in the modeling of electron transport in solids for many applications such as electron-probe microanalysis [1–3], Auger-electron spectroscopy [4] and dimensional metrology in the scanning electron microscope [5–7]. In Monte Carlo simulations for these and other applications, the continuous slowing-down approximation has often been utilized in which it is assumed that the electron energy is a continuous function of the trajectory length in a material. This approach is convenient because data for differential cross sections as a function of energy loss are not required and because computation time is reduced if inelastic-scattering events are not individually simulated [4]. It is, however, necessary to know the dependence of the SP on electron energy in solids over a wide energy range, typically 100 eV to 30 keV.

SPs for Monte Carlo simulations have often been determined from the Bethe SP equation [8–10] and data for one material parameter, the mean excitation energy [11]. This equation is expected to be valid for electron energies greater than about 10 keV or for energies much greater than the largest K-shell binding energy in the material of interest. SPs calculated from the Bethe equation are available from a National Institute of Standards and Technology (NIST) database for electron energies of 10 keV and above [12]. Several empirical SP equations [13–15] have been developed for energies less than 10 keV but their use is restricted to materials for which needed parameters are known. Furthermore, it is difficult to adapt these equations to energies less than several hundred eV. Although experimental determinations of the SP over a range of energies are available for a limited number of materials [16], different sets of data for a particular material can disagree significantly.

Tanuma et al. [17,18] recently reported SPs for 41 elemental solids over the 100 eV to 30 keV energy range that were calculated from experimental optical data using the Penn algorithm [19]. Jablonski et al. [20] analyzed these results and proposed an empirical predictive SP formula for the 200 eV to 30 keV energy range.

We report a new analysis of the calculated SPs of Tanuma et al. [17,18] and propose a new SP formula that can be applied over the 100 eV to 30 keV energy range. Our analysis of the SP energy dependence for each solid was carried out using Fano plots [21,22] in which the product of the SP, $S$ and electron energy, $E$, is plotted versus energy on a logarithmic scale.

The nonrelativistic Bethe SP equation is [8–10]

$$S = \frac{784.6Z\rho}{EA}\ln\left(\frac{1.166E}{I}\right) \quad (\text{in eV/Å}), \tag{1}$$

* Corresponding author. Tel.: +81 29 859 2725; fax: +81 29 859 2729.
*E-mail address:* kumagai.kazuhiro@nims.go.jp (K. Kumagai).

0168-583X/$ - see front matter © 2008 Elsevier B.V. All rights reserved.
doi:10.1016/j.nimb.2008.10.094

where $Z$ is the atomic number, $\rho$ is the density (in g/cm$^3$), $A$ the atomic weight, $I$ is the mean excitation energy (in eV) and $E$ is expressed in eV. It is convenient to rearrange Eq. (1) for a Fano plot

$$SEk = \ln(1.166/I) + \ln E, \tag{2}$$

where $k = A/784.6Z\rho$. If the Bethe equation were valid over a given energy range, the corresponding plot of $SEk$ versus $\ln E$ would be linear with a slope of unity.

As examples, the solid circles in Fig. 1(a) and (b) show Fano plots for Si and Au in which $SEk$ is plotted against $E$ on a logarithmic scale. These plots were prepared with SPs calculated from optical data [17,18] (hereafter referred to as optical SPs). Optical SPs are included for energies between 10 eV and 100 eV to illustrate trends, although these SPs should be regarded only as semi-quantitative guides [18].

The dashed lines in Fig. 1(a) and (b) show plots of the product $SEk$ from Eq. (2) (with $I$ values as recommended in [11]) as a function of $E$. While the Fano plots from the optical SPs for Si and Au show linear regions, for energies greater than 500 eV for Si and greater than 10 keV for Au, their slopes are larger than those for the Fano plots from the Bethe equation. At lower energies, $SEk$ values from the optical SPs gradually decrease and approach zero with decreasing energy. That is, as is well known, the Bethe SP equation is not valid for energies less than about 10 keV [11–18].

The slopes of the Fano plots for Si and Au from the optical SPs are shown as solid circles in Fig. 1(c) and (d) as a function of electron energy. We see that these slopes show a series of steps with increasing energy. Each of these steps corresponds to contributions to the stopping power from a particular electronic shell (valence-band, L-shell and K-shell for Si in Fig. 1(c) and valence-band, O-shell, N-shell and M-shell for Au in Fig. 1(d)). As the energy increases to our limit of 30 keV, the slopes approach unity as expected from Eq. (2).

We have chosen to fit plots of slopes of Fano plots using the Hill equation [23]. In principle, any sigmoid function would be appropriate but the Hill equation is a simple expression that can be easily integrated. This equation can be expressed as

$$y = a\frac{E^n}{E^n + b^n}, \tag{3}$$

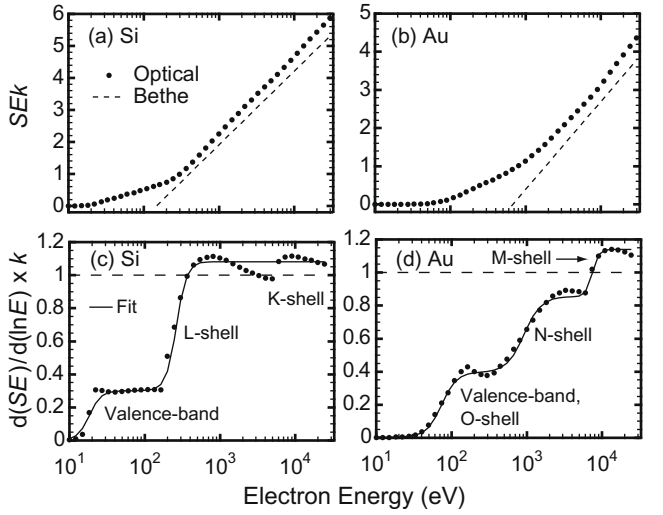


**Fig. 1.** Fano plots ((a) and (b)) (based on Eq. (2)) and slopes of Fano plots ((c) and (d)) for Si and Au. The closed circles are derived from optical SPs and the dashed lines in (a) and (b) show values from the Bethe equation (Eq. (1)). The solid lines in (c) and (d) show fits to the Fano plot slopes with Eq. (4), and the dashed lines indicate the value (unity) expected from the Bethe equation.

where $a$ is the height of a step, $b$ is the electron energy at the center of a step and $n$ determines the steepness of the slope at a step. Although this equation is empirical, we can associate physical meanings to the parameters $a$, $b$ and $n$.

If a plot of the slope of a Fano plot for a given element has $m$ steps, we can describe the plot by

$$k\frac{\mathrm{d}(SE)}{\mathrm{d}\ln E} = \sum_{i=1}^{m} a_i \frac{E^{n_i}}{E^{n_i} + b^{n_i}}. \tag{4}$$

The solid lines in Fig. 1(c) and (d) show fits of the Fano plot slopes for Si and Au with Eq. (4), and we see reasonable agreement. Although there are some deviations of the fits from the plotted points (e.g. for Si above 600 eV), these do not significantly affect our later results. We find it more convenient to fit the Fano plots directly with a function that is an integral of Eq. (4)

$$SEk = \sum_{i=1}^{m} \left[\frac{a_i}{n_i} \ln\left(\frac{E^{n_i} + b^{n_i}}{b^{n_i}}\right)\right]. \tag{5}$$

We have fitted Fano plots with the optical SPs for our group of 41 elemental solids with Eq. (5). The solid lines in Fig. 2(a) and (b) show examples of these fits for Si and Au. Direct comparisons of the optical SPs and the values derived from the fits with Eq. (5) are shown in Fig. 2(c) and (d), where we see excellent agreement with the optical SPs. The root-mean-square (rms) difference of the fitted values from the optical values of $SE$ were 0.8% for Si and 1.0% for Au. The average of the rms differences for the 41 solids was 1.0% over the 100 eV to 30 keV energy range. This value is superior to those found in fits of the optical SPs with other empirical equations over the same energy range: 4.5% with the Joy–Luo equation [14] and 3.0% with the Jablonski–Tanuma–Powell [20] equation.

Our new expression for the SP can be obtained by rearranging Eq. (5)

$$S = \frac{784.6Z\rho}{EA}\sum_{i=1}^{m}\frac{a_i}{n_i}\ln\left[1 + \left(\frac{E}{b_i}\right)^{n_i}\right] \quad (\text{in eV/Å}). \tag{6}$$

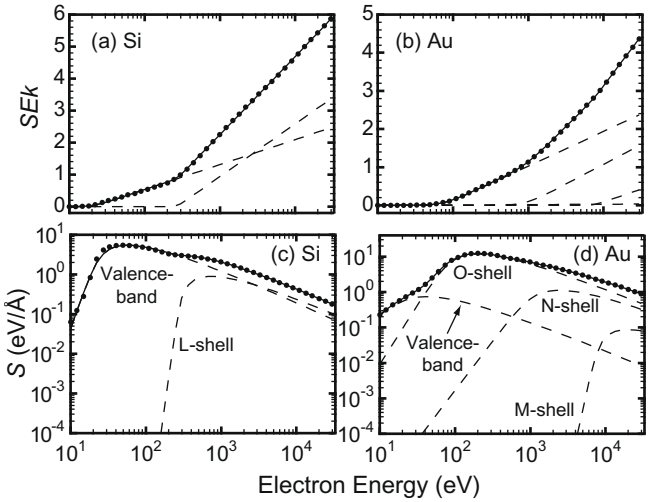


**Fig. 2.** Partial contributions of each electronic shell to the Fano plots and stopping powers for Si and Au. The solid lines show fits of the Fano plots with the optical SPs (solid circles) using Eq. (5) for (a) Si and (b) Au. The solid circles in (c) and (d) are the optical SPs and the solid lines show the results of the fits. The dashed lines show the contributions of valence-band and inner-shell excitations to $SEk$ and $S$. The parameters from the fit for Si are $a_1 = 0.301$, $b_1 = 18.3$ (eV) and $n_1 = 5.49$ for the valence-band, and $a_2 = 0.781$, $b_2 = 262$ (eV) and $n_2 = 6.33$ for the L-shell. The parameters from the fit for Au are $a_1 = 0.00549$, $b_1 = 16.9$ (eV) and $n_1 = 2.92$ for the valence-band, $a_2 = 0.390$, $b_2 = 74.2$ (eV) and $n_2 = 4.35$ for the O-shell, $a_3 = 0.458$, $b_3 = 918$ (eV) and $n_3 = 3.79$ for the N-shell, and $a_4 = 0.286$, $b_4 = 7386$ (eV) and $n_4 = 10.7$ for the M-shell.